

# Scalable Polymer based Ferrite Composites with Matching Permeability and Permittivity for High-Frequency Applications

Yunqi Wang<sup>1,\*</sup>, Eleanor Edwards<sup>1</sup>, Ian Hooper<sup>2</sup>, Nathan Clow<sup>3</sup> and Patrick S. Grant<sup>1</sup>

- <sup>1.</sup> Department of Materials, University of Oxford, Parks Road, Oxford, OX1 3PH, UK  
<sup>2.</sup> Electromagnetic and Acoustic Materials Group, Department of Physics and Astronomy, University of Exeter, Stocker Road, Exeter, EX4 4QL, UK  
<sup>3.</sup> Defence Science and Technology Laboratory, Salisbury, SP4 0JQ, UK

**Abstract** Materials with relatively high and equal permeability and permittivity are promising for applications in telecommunications but so far few practical candidates have been identified. In this work, functional composites consisting of epoxy resin and Ni<sub>0.4</sub>Zn<sub>0.6</sub>Fe<sub>2</sub>O<sub>4</sub> ferrite particles have been fabricated by a scalable and flexible casting route. It has been experimentally demonstrated that at frequencies in the hundred MHz range, the composite with ferrite loading of 53 vol. % can achieve broadband impedance matching to free space with a refractive index of approximately 6, giving less than 0.03% reflection and over 96% transmission of incident radiation. These results indicate a more flexible route to the fabrication of impedance matched materials for antenna miniaturisation, which has been demonstrated by the casting of the impedance matched composite into hemispheres suitable for electrically small antennas.

## 1 Introduction

Materials that allow no reflection and complete power transmission of incident radiation at discontinuities or interfaces are in demand for advances in stealth technology, anti-reflection coating, and antenna miniaturization [1, 2]. To realize zero reflection, materials used in device construction must have impedance ( $Z = Z_0 \sqrt{\mu' / \epsilon'}$ , where  $Z$  and  $Z_0$  are the impedance of the material and free space respectively,  $\mu'$  and  $\epsilon'$  are the real parts of the relative permeability and permittivity of the

materials) match to that of free space, so that  $\mu'$  and  $\epsilon'$  must be equal. However, no naturally occurring monolithic materials have been found so far that satisfy impedance matching conditions.

Whilst it has been suggested that a chessboard structure comprising a periodic array of magnetic and dielectric media could provide equal values of relative real permeability and permittivity [3, 4], these approaches present practical manufacturing and scaling difficulties so that technological implementation has been limited. Alternatively, impedance-matched materials can be achieved through control of the microstructural porosity and grain size of complex nano-ferrites with compositions such as Ni<sub>0.35</sub>Zn<sub>0.35</sub>Co<sub>0.2</sub>Mn<sub>0.05</sub>Cu<sub>0.05</sub>Fe<sub>1.98</sub>O<sub>4</sub> [5], Ni<sub>0.5</sub>Zn<sub>0.3</sub>Co<sub>0.2</sub>Fe<sub>2</sub>O<sub>4</sub> [6, 7], and Ni<sub>0.855</sub>Cu<sub>0.1</sub>Zn<sub>0.025</sub>Co<sub>0.02</sub>Fe<sub>1.98</sub>O<sub>4</sub> [8] via appropriate heat treatment. Similarly, manipulations of the stoichiometry of Ni<sub>0.95-x</sub>Zn<sub>x</sub>Co<sub>0.05</sub>Fe<sub>1.90</sub>Mn<sub>0.02</sub>O<sub>4</sub> ferrites can achieve variations in relative permeability and the impedance can be matched with  $x = 0.10$ - $0.25$ , but only for frequencies between 2-30 MHz [9]. These studies confirm the possibility of realizing impedance matched materials artificially but rely on the use of sintered ceramics with often complex and difficult to control compositions, prepared by intricate co-precipitation and heat treatments that leads to comparatively high-cost.

As an alternative, polymer composites are considered attractive owing to their light-weight, deformability, and ease of tunable physiochemical properties. It has been demonstrated that through smart manipulation of the composition, size, and morphology of the fillers in composites, improved electromagnetic absorption behaviour can be

\* Author to whom correspondence should be addressed. Electronic mail: yunqi.wang@materials.ox.ac.uk.

achieved [10-12]. In this study, a simple polymer-based composite approach with matching permeability and permittivity could be attractive because of the potential for large-scale manufacturing, and their ability to be fabricated into various 3D shapes and real components, overcoming the disadvantages of complex composition ferrite ceramics. In a recent work [13], we modified the particle morphology of ferrite and Fe powders by ball milling, which then subsequently embedded in an epoxy matrix by casting, increased the cut-off frequency. This approach was used to show how a useful magnetic response of the easy-to-process composite could be maintained to higher frequency. In this paper we use a similar process route but focus not on frequency extension but impedance matching, although in principle the approaches could be combined. We show ferrite composites of refractive index  $\sim 6$  that are broadband impedance matched to free space, and experimentally demonstrate this material allows more than 96% power transmission and less than 0.03% power reflection to approximately 100 MHz. We present measurements of the frequency-dependent complex permeability and permittivity of epoxy based composites using a stripline technique [14] for frequencies between 5 MHz to 2 GHz, and demonstrate both impedance-matching for a ferrite loading of 53 vol.%, and the ability to produce practical antenna geometry with ease.

## 2 Experimental

The polymer matrix for the composites was commercial epoxy embedding medium (Epon<sup>TM</sup> 812 substitute) with two different hardeners of 2 dodecenylsuccinic anhydride (DDSA) and methylnadic anhydride (MNA) (Sigma Aldrich Ltd. UK). The ferrite filler was sintered NiZn ferrite powder (F16 MagDev Ltd. UK) with composition  $\text{Ni}_{0.4}\text{Zn}_{0.6}\text{Fe}_2\text{O}_4$  (standard pattern ref. No. 01-077-9718) by X-ray diffraction (Simens D5000). The range of particle sizes spanned from 1  $\mu\text{m}$  to 10  $\mu\text{m}$  determined by laser diffraction (Mastersizer 2000, Malvern Instruments Ltd.). NiZn ferrite powder and epoxy were mixed together using 5 min ultrasonication in an ice bath

and then cured at 60 °C overnight. Prolonged stirring and ultrasonication in an ice bath were necessary to disperse the highest ferrite loadings into an acceptably uniform distribution of particles within the epoxy matrix. Although not explored in this study, higher loadings with acceptable dispersions might be facilitated using surface-initiated-polymerization methods [15, 16]. Composites with 0, 11, 32, 53 and 61 vol.% NiZn ferrite filler were prepared, with 61 vol.% the highest loading that could be easily cast due to the increasing viscosity. For an even higher loading, cold-pressing can achieve up to 80 vol.% ferrite in a polymer matrix, but has greater geometric restrictions [17].

The magnetic and dielectric properties of the composites were measured using a standard stripline technique in which a central flat conducting line is symmetrically bounded by two ground planes and supports a transverse electromagnetic (TEM) waveguide mode. The stripline rig was connected to a calibrated vector network analyzer (VNA) and used to measure the complex reflection and transmission amplitude coefficients of two identical blocks of materials placed symmetrically above and below the conducting line. The complex permeability and permittivity of the material were then extracted according to the method of Nicolson, Ross and Weir [18, 19]. The dimensions of the samples were: length = 43 mm, width = 15 mm, and thickness = 4.8 mm, in order to fit tightly within the stripline rig to avoid air gaps all samples were machined with extra care. The electromagnetic wave propagated along the direction of sample width during measurements.

## 3 Results and discussion

As scanning electron microscopy (840F SEM, JEOL) image of a cross-section of a 53 vol. % ferrite casting is shown in Fig. 1. Many such cross-section indicated an adequate homogeneity of ferrite filler dispersion with no large agglomerates; the cross-sections also suggested that any entrapped air bubbles were comparatively rare.

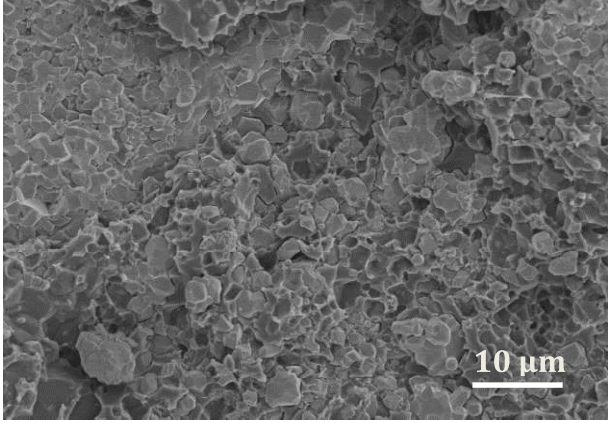


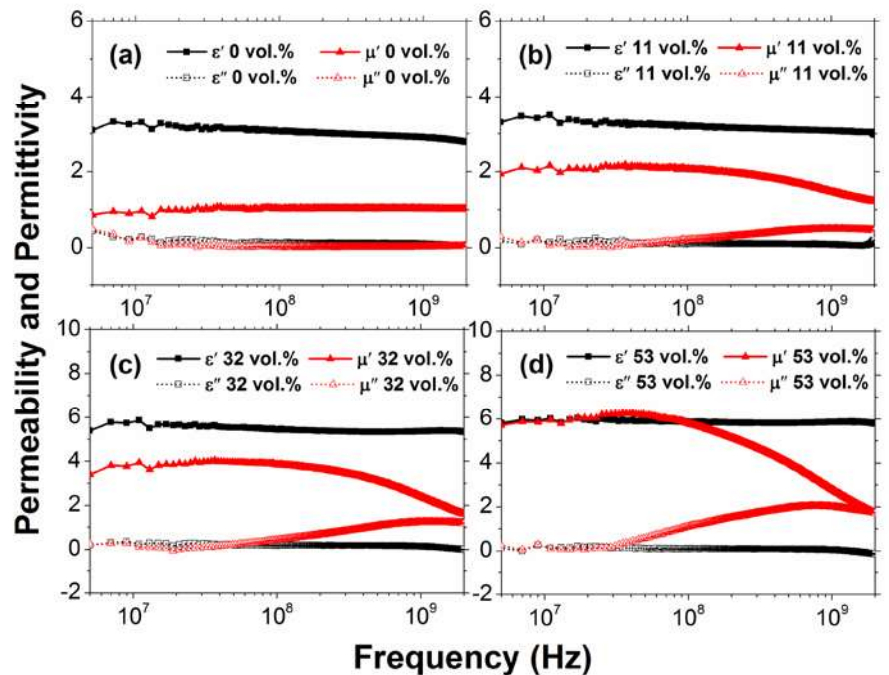
**Fig. 1** SEM image of the fractured cross-section of a NiZn ferrite/epoxy composite with a 53 vol.% ferrite loading

The frequency responses of the complex permeability and permittivity from 5 MHz to 2 GHz at each volume fraction are plotted in Fig. 2. For polycrystalline ferrite, the magnetization mechanisms are generally considered to be spin rotation in the magnetic domains and domain wall motion [20, 21]. In Fig. 2a for no ferrite addition, the real permeability  $\mu'$  remains at approximately 1 over the measured frequency range, as expected, and the permittivity was constant at  $\sim 3$ . Figs. 2b-d

show the effects of 11 vol. %, 32 vol. % and 53 vol. % NiZn ferrite respectively, with the low frequency  $\mu'$  response approximately constant before decreasing as the frequency increased. The imaginary permeability  $\mu''$  remained relatively low at 0.01 to 0.2 below several tens of megahertz, but increased at higher frequencies to form a broad peak with a maximum at around the frequency at which  $\mu'$  dropped to approximately half its plateau value (Fig. 2b-d) [5, 22]. The increase of  $\mu''$  was mainly due to domain wall motion no longer following the applied alternating magnetic field [23].

In order to consider if these variations conform to expected behaviours, a magnetic circuit model [24] was applied. This model accounted for the way in which the non-magnetic matrix creates magnetic poles on the surface of ferrite grains/particles under an applied magnetic field, thus producing demagnetizing fields, which lead to a decrease in permeability. The magnitude of the demagnetizing field is closely related to the ferrite grain/particle size and non-magnetic phase characteristic. The composite static permeability  $\mu_s$  that corresponds to the real permeability at frequencies far below any resonant response is assumed to vary according to [24]:

**Fig. 2** Frequency dispersions of complex permeability and permittivity for samples with **a** 0 vol.%, **b** 11 vol.%, **c** 32 vol.%, and **d** 53 vol.% of NiZn ferrite loadings. The slight drop in permittivity at the lowest frequency was due to measurement instrument working frequency limit



$$\mu_s = \frac{\mu_i(1 + (\delta/D))}{1 + \mu_i(\delta/D)} = 1 + \frac{\mu_i - 1}{1 + \mu_i(\delta/D)} \quad (1)$$

where  $\mu_i$  is the intrinsic static permeability of a ferrite without any defects,  $\delta$  is the distance between grains/particles (in other words, it is the thickness of non-magnetic phases), and  $D$  is the grain/particle size. With increasing vol.% of ferrite, the corresponding decrease in adjacent particle distance  $\delta$  will lead to a decrease in the ratio  $\delta/D$ , and thus increasing static permeability  $\mu_s$ . Assuming that the ferrite particles were spherical and homogeneously distributed in an epoxy matrix (a reasonable assumption consistent with the observed microstructure), the experimentally derived value of  $\mu_s$  taken at frequency of 10 MHz can be plotted against the  $\delta/D$  ratio derived from the volume fraction of ferrite, as shown in Fig. 3. Using a best-fit of  $\mu_i = 40$  (which is a sensible reduction from the ferrite manufacturer's supplied value of  $\mu_i = 120$  for identical material but in sintered "bulk" [25-27]), Fig. 3 shows that static permeability increased with decreasing adjacent particle distance, in close agreement with Eq. (1).

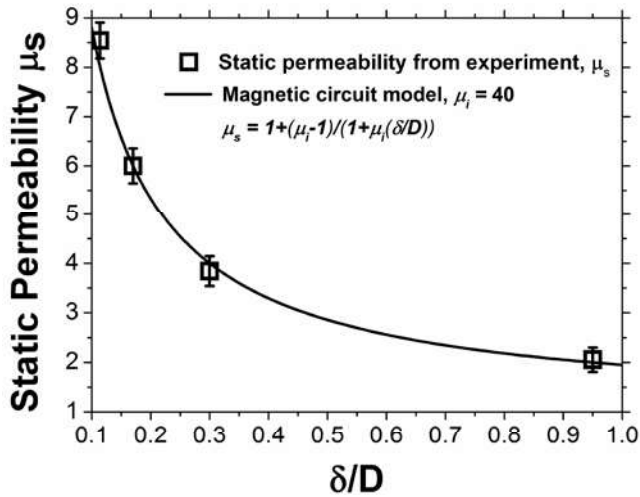


**Fig. 3** The experimentally measured static permeability  $\mu_s$  (as obtained from Fig. 2) as a function of the particle separation ratio  $\delta/D$ , assuming homogeneously dispersed, spherical ferrite filler

The permittivity response of NiZn ferrites is provided by atomic and electronic polarization,

which was largely independent of frequency in the range 5 MHz to 2 GHz used in this study, with both real and imaginary permittivities almost constant over the range.

Because permeability increased more rapidly than permittivity due to the greater inherent permeability of the ferrite filler, at 53 vol.% ferrite in Fig. 2d the permeability and permittivity were approximately equal, and remained so until a cut-off frequency at ~100 MHz, beyond which  $\mu'$  began to reduce. Modification of particle morphology was previously studied to increase the cut-off frequency [13], which may provide possibility to further extend impedance match bandwidth.

The Lichtenecker mixing formula [28] has proven to be a flexible and widely applicable approach for estimating the effective permeability and permittivity medium of composite systems, was subsequently derived from Maxwell's equations by Simpkin [29]. As shown, it provides a useful fit to the data and correctly identified the ferrite fraction for impedance matching. The general formula for a two-component mixture is:

$$\log(\Psi_{eff}) = f \log(\Psi_i) + (1 - f) \log(\Psi_m) \quad (2)$$

where  $\Psi_{eff}$ ,  $\Psi_m$  and  $\Psi_i$  represent either the complex permeability or permittivity of the effective medium, the matrix and the fillers respectively, and  $f$  is the volume fraction of filler. Fig. 4 shows a direct comparison of experimental data  $\mu'_{eff}$  and  $\epsilon'_{eff}$  for the ferrite composites at 10 MHz along with their predicted values using Eq. (2) by substituting into the matrix and filler properties  $\mu'_m = 1$ ,  $\epsilon'_m = 3$ ,  $\mu'_i = 40$  (as used in Fig. 3) and  $\epsilon'_i = 13$ , which were based on data supplied by ferrite manufacturer. A frequency of 10 MHz was chosen because the measured complex permeability and permittivity were largely non-dispersive at this frequency. The experiment and theory shows reasonable agreement over the range. Deviations from theory may arise due to agglomeration effects, limited porosity (air bubbles), and lack of precise control over volume fraction. Fig. 4 shows the real permeability and permittivity curves predicted by the Lichtenecker formula were coincident at ~6 for a ferrite volume



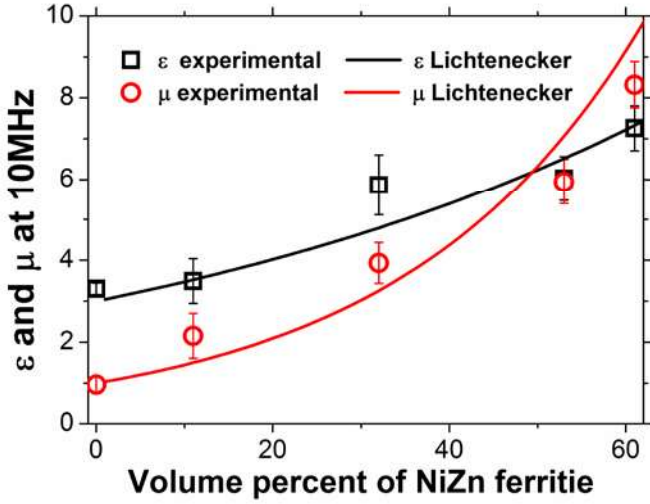
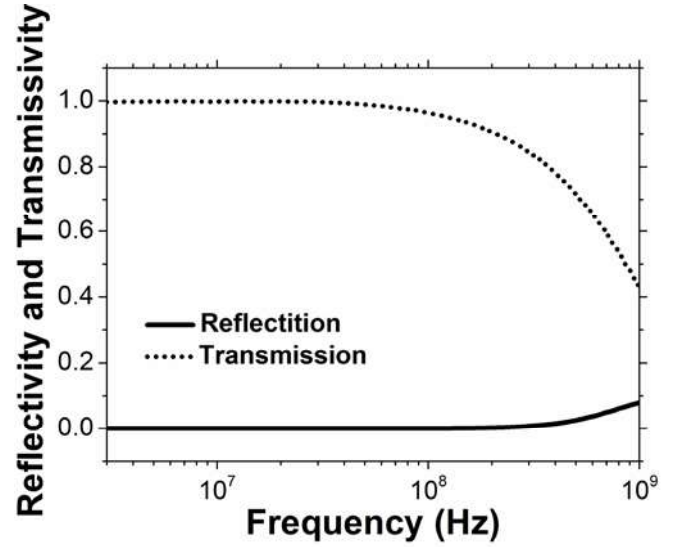


**Fig. 4** The effective real permeability and permittivity at 10 MHz as a function of volume percent NiZn ferrite in an epoxy matrix and the predicted dependence with volume fraction of ferrite using the Lichtenecker approximation

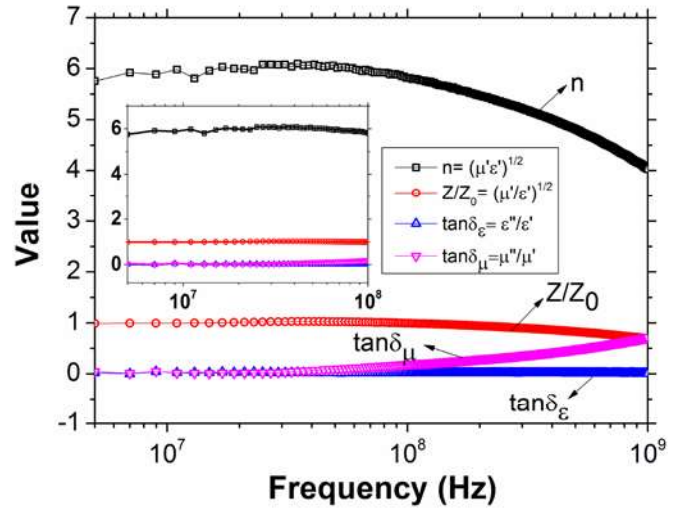
around 50%, which was in accord with our experimental results.

Fig. 5 shows the experimentally measured reflectivity and transmissivity from the  $\text{Ni}_{0.4}\text{Zn}_{0.6}\text{Fe}_2\text{O}_4$ /epoxy composite with 53 vol. % ferrite loadings as a function of frequency. The material transmitted more than 96% of the incident power, while maintaining a reflection coefficient of less than 0.03% for frequencies up to 100 MHz, showing superior performance over a recent report on array structured impedance matched materials that have 80% transmission and 0.3% reflection at 100 MHz for only orthogonal linear polarized radiation [30]. The transmission reduced significantly above 100 MHz due to losses caused by magnetic resonance.

The extracted values of refractive index, reduced impedance, and magnetic and dielectric loss tangents of the 53 vol. % ferrite loading composite are plotted in Fig. 6. The permeability and permittivity were almost equal up to a frequency of approximately 100 MHz, which resulted in an impedance ( $Z = \sqrt{\mu_0\mu'/\epsilon_0\epsilon'} = Z_0\sqrt{\mu'/\epsilon'} = Z_0$ ) close to that of free space and a refractive index of approximately 6.



**Fig. 5** Experimentally determined reflectivity and transmissivity from  $\text{Ni}_{0.4}\text{Zn}_{0.6}\text{Fe}_2\text{O}_4$ /epoxy composite with 53 vol. % ferrite



**Fig. 6** Refractive index, reduced impedance, dielectric and magnetic loss tangents of a 53 vol. % ferrite/epoxy composites. The inset shows the zoom in results in the range 5-100 MHz

For antenna miniaturization applications, broadband impedance matched materials with high refractive index  $n=(\mu'\epsilon')^{1/2}$  are preferable since the electrical length of an antenna is the product of its physical length and the antenna medium refractive index [2]. Hence, the physical

dimension of an antennas made from this material could be reduced by a factor of  $\sim 6$  over materials with  $n = 1$  without changing the effective electrical length. In addition, the materials with equal permeability and permittivity minimize the antenna problems of strong field confinement [31] and mismatched impedance with free space.

Any electrically small antenna will tend to have a narrow operational bandwidth, and in order to maximize the bandwidth, the antenna can be enclosed within a spherical volume such that it efficiently diminishes the fields within the radiation sphere circumscribing the antenna [32, 33]. There have been a wide variety of novel geometrical designs enabling resonant antenna elements to be encased within such an electrically small volume [34-37], but easily processable materials with acceptable mechanical properties become crucial in realizing these designs in practice. In particular, it is difficult and expensive to achieve various curved surface designs using comparatively brittle and difficult to machine bulk ferrites. In contrast, it was straight-forward to cast the composites into desired geometries, even at high ferrite loadings. For example, Fig. 7 shows an impedance-matched epoxy-53%NiZn ferrite cast into a hemisphere according to the design of an electrically small folded spherical helix antenna [34].



**Fig. 7** Hemisphere shells with 5 cm in diameter cast from an impedance-matched epoxy-53%NiZn ferrite composite

## 4 Conclusions

In this study, a simple mould casting method for producing ferrite/epoxy composites has been developed that allows materials with a matched permeability and permittivity of  $\sim 6$  and reflection less than 0.03% over the frequency range 5-100 MHz to be produced using 53 vol.%  $\text{Ni}_{0.4}\text{Zn}_{0.6}\text{Fe}_2\text{O}_4$  powder. The experimental results for both permeability and permittivity accord well with the Lichtenecker formula, enabling it to be used to explore impedance matched materials with a variety of different filler materials via a composite approach. The epoxy based composites are easy to process, scalable, machinable and can be directly formed into 3D geometries, with similar or improved performance over monolithic, complex composition sintered ferrites, providing more freedom for antenna miniaturisation. The results show the utility of a generic approach for achieving impedance matched materials, without the need for subtle thermal manipulations of complex composition materials. Further it is suggested that any magnetic material with permeability higher than permittivity can provide an impedance match by tuning of the material fractions in the composite fabrication route.

**Acknowledgements** The authors would like to thank the UK Engineering and Physical Sciences Research Council (QUEST Programme Grant EP/I034548/1) and the UK Defence Science and Technology Laboratory for financial support.

© Crown Copyright, Defence Science and Technology Laboratory UK.

## References

1. L. B. Kong, Z. W. Li, G. Q. Lin, and Y. B. Gan, *J. Am. Ceram. Soc.* 90, 3106 (2007)
2. M. L. S. Teo, L. B. Kong, Z. W. Li, G. Q. Lin, and Y. B. Gan, *J. Alloy Compd.* 459, 557 (2008)
3. W. Yu, R. Mittra, and D. H. Werner, *IEEE Microw. Guided Wave Lett.* 9, 496 (1999).
4. W. Yu, D. H. Werner, and R. Mittra, *IEEE Microw. Guided Wave Lett.* 10, 128 (2000)

5. A. Thakur, P. Thakur, and J. -H. Hsu, *Scripta Mater.* 64, 205 (2011)
6. A. Thakur, A. Chevalier, J. -L. Mattei, and P. Queffelec, *J. Appl. Phys.* 108, 014301 (2010)
7. D. Souriou, J. -L. Mattei, A. Chevalier, and P. Queffelec, *J. Appl. Phys.* 107, 09A518 (2010)
8. H. Su, X. Tang, H. Zhang, Y. Jing, F. Bai, and Z. Zhong, *J. Appl. Phys.* 113, 17B301 (2013)
9. L. B. Kong, Z. W. Li, G. Q. Lin, and Y. B. Gan, *IEEE Trans. Magn.* 43, 6 (2007)
10. Q. He, T. Yuan, X. Zhang, X. Yan, J. Guo, D. Ding, M. A. Khan, D. P. Young, A. Khasanov, Z. Luo, J. Liu, T. D. Shen, X. Liu, S. Wei, and Z. Guo, *J. Phys. Chem. C* 118, 24784 (2014)
11. J. Zhu, S. Wei, N. Haldolaarachchige, D. P. Young, and Z. Guo, *J. Phys. Chem. C* 115, 15304 (2011)
12. Z. Guo, S. Park, H. T. Hahn, S. Wei, M. Moldovan, A. B. Karki, and D. P. Young, *J. Appl. Phys.* 101, 09M511 (2007)
13. Y. Wang and P. S. Grant, *Appl. Phys. A* 117, 477 (2014)
14. W. Barry, *IEEE Microwave Th. Tech.* 34, 80 (1986)
15. Z. Guo, S. Park, S. Wei, T. Pereira, M. Moldovan, A. B. Karki, D. P. Young, and H. T. Hahn, *Nanotechnology* 18, 335704 (2007)
16. Z. Guo, S. -E. Lee, H. Kim, S. Park, H. T. Hahn, A. B. Karki, and D. P. Young, *Acta Mater.* 57, 267 (2009)
17. L. Parke, I. R. Hooper, R. J. Hicken, C. E. J. Dancer, P. S. Grant, I. J. Youngs, J. R. Sambles, and A. P. Hibbins, *APL Mater.* 1, 042108 (2013)
18. W. W. Weir, *Proc. IEEE* 62, 33 (1974)
19. A. M. Nicolson and G. F. Ross, *IEEE Trans. Instrum. Meas.* 19, 377 (1970)
20. A. Globus, *J. Phys. Colloques.* 38, C1-1-C1-15 (1977)
21. H. Su, H. Zhang, X. Tang, and Y. Jing, *J. Appl. Phys.* 103, 093903 (2008)
22. R. E. Alley Jr., *Bell Syst. Tech. J.* 32, 5 (1953)
23. H. Dawoud, S. Shaat, and An-Najah, *Univ. J. Res. (N.Sc.)* 20, 87 (2006)
24. M. T. Johnson and E.G. Visser, *IEEE Trans. Magn.* 26, 1987 (1990)
25. M. Anhalt, *J. Magn. Magn. Mater.* 320, 366 (2008).
26. Z. W. Li, G. Q. Lin, Y. P. Wu, and L. B. Kong, *J. Magn. Magn. Mater.* 321, 734 (2009)
27. N. E. Kazantseva, J. Vilcakova, V. Kresalek, P. Saha, I. Sapurina, and J. Stejskal, *J. Magn. Magn. Mater.* 269, 30 (2004)
28. K. Lichtenecker and K. Rother, *Z. Phys.* 32, 255 (1931)
29. R. Simpkin, *IEEE Trans. Microwave Theory Techn.* 58, 3 (2010)
30. L. Parke, I. J. Youngs, A. P. Hibbins, and J. R. Sambles, *Appl. Phys. Lett.* 104, 221905 (2014)
31. H. Mosallaei and K. Sarabandi, *IEEE Trans. Antennas Propag.* 52, 1558 (2004)
32. L. J. Chu, *J. Appl. Phys.* 10, 1163 (1948)
33. H. A. Wheeler, *Proc. IRE* 47, 1325 (1959)
34. S. R. Best, *IEEE Trans. Antennas Propag.* 52, 953 (2004)
35. S. R. Best, *IEEE Antennas Propag. Mag.* 46, 9 (2004)
36. S. R. Best, *IEEE Trans. Antennas Propag.* 53, 502 (2005)
37. S. R. Best, *IEEE Antennas Propag. Mag.* 53, 1047 (2005)